

Optimal Operation of a Tubular Chemical Reactor

MARK R. NEWBERGER and ROBERT H. KADLEC

University of Michigan, Ann Arbor, Michigan 48104

A theoretical and experimental study was conducted on the optimal steady state operation of a jacketed, tubular, liquid-phase reactor in which consecutive second-order reactions occurred in turbulent flow. To verify the proposed mathematical model, diethyl adipate was saponified with sodium hydroxide in aqueous solution. The 150 ft. long reactor jacket was divided into 5, 30 ft. sections. Hot water flow rates in the jacket sections were chosen to maximize the concentration of monoethyl adipate ion at the reactor exit. The plug-flow model and a position-dependent heat transfer coefficient accurately described temperature and concentration profiles. The Pontryagin maximum principle was used to choose idealized reactor temperature and wall heat flux profiles which would maximize the exit concentration of monoester. The maximum principle was shown to be an effective tool for this type of reactor optimization. A technique is given for optimizing more complex reaction systems.

A natural application of high speed computation in chemical engineering has been the optimal design and operation of processing equipment. In recent years application of variational and numerical search methods has shown that the performance of many chemical reactors may be improved by operating in a nonisothermal fashion (1, 2, 4, 6 to 8, 11). These studies have for the most part been confined to mathematical models and computer simulation. This work concerns the optimal operation of a jacketed, unpacked, tubular reactor in which consecutive second-order liquid-phase reactions occur in turbulent flow (9). The reaction considered is the saponification of diethyl adipate with sodium hydroxide.

The first objective of this research was to model effectively the tubular reactor by comparing experimental concentrations and temperature profiles with predictions of various models. Numerical search techniques were then employed to maximize yields of monoethyl adipate at the reactor exit. Optimal operation was also verified experimentally.

The second objective of this research was to obtain optimal constrained temperature and wall heat flux profiles for consecutive first- and second-order reactions occurring in a fixed length reactor, and for which $E_1 > E_2$. The Pontryagin maximum principle was employed to determine optimal profiles for several objective functions. Comparison of yields from the idealized reactor (amenable to study with the maximum principle) with yields from the experimental system indicated that the maximum principle is useful in obtaining an upper bound on yields in real reactors.

DESCRIPTION OF EXPERIMENTAL SYSTEM

The reactor system, shown in Figure 1, consisted of a jacketed tubular reactor, storage drums for diethyl adipate and sodium hydroxide solutions, feed and hot water flowmeters and

pumps, a feed temperature control system, 15 iron-constantan thermocouples for monitoring feed and reactor temperatures, a 0.1-mv. potentiometer for reading thermocouple output, and five sampling taps.

The reactor, shown in Figure 2, consisted of 10, 15-ft. lengths of 0.25-in. O.D. copper tubing concentric with 0.625-in. O.D. tubing. Inner tubes were connected in series. Pairs of outer tubes were connected forming five shell sections. The shell was insulated with fiberglass wrapping. Hot water flow through each shell section controlled reactant temperature. The reactant flow rate was constant at 197 lb./hr. with inlet concentrations at 0.018 mole/liter diethyl adipate and 0.05 mole/liter sodium hydroxide. Shell water flow rates varied from 0 to 600 lb./hr. Tube and shell inlet temperatures were approximately 80° and 180°F.

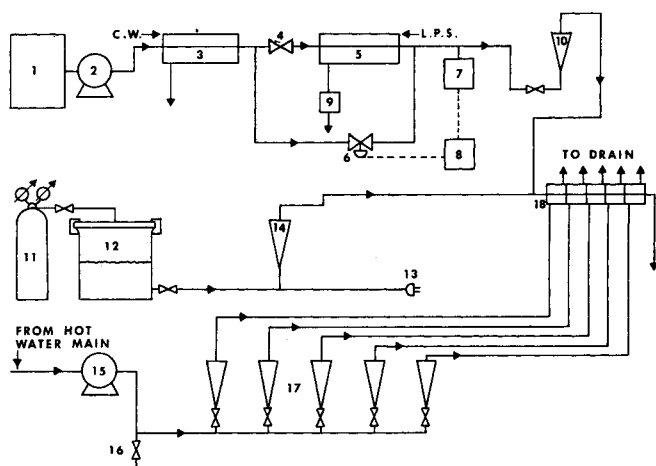


Fig. 1. Schematic drawing of reactor system. 1. Ester feed drum, 55-gal. polyethylene-lined steel. 2. Ester feed pump, Oberdorfer bronze gear pump, Model 1000, 1.51/min. at 80 lb. sq. in. gauge, 800 rev./min. 3. Ester precooling heat exchanger. 4. Pressure equalizing 1/8-in. needle valve. 5. Ester temperature control heat exchanger, steam. 6. Bypass control valve, annin. 7. Pneumatic temperature transducer, Taylor. 8. Two-mode recorder, controller, Foxboro. 9. Steam trap, Yarway. 10. Ester rotameter, Brooks. 11. Nitrogen gas cylinder. 12. Sodium hydroxide feed tank, polyethylene-lined steel. 13. Sodium hydroxide thermocouple. 14. Sodium hydroxide rotameter, Brooks. 15. Hot water pump, Oberdorfer bronze gear pump, Model 4000. 16. Hot water bypass valve. 17. Hot water rotameters, Brooks. 18. Tubular reactor.

Mark R. Newberger is with American Cyanamid Company, Engineering and Construction Division, Wayne, New Jersey 07470.

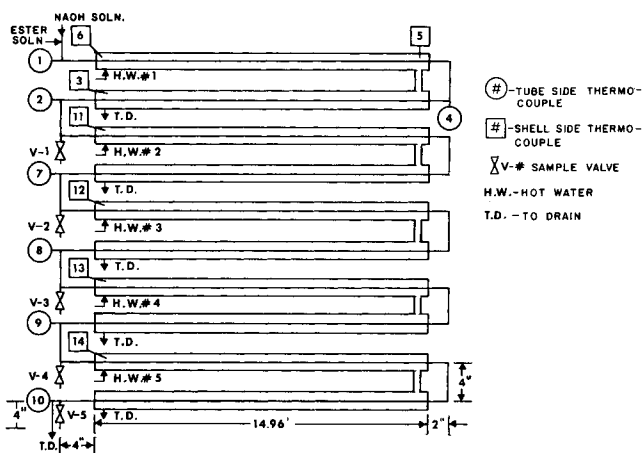


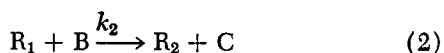
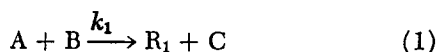
Fig. 2. Schematic drawing of tubular reactor.

The dimensions of the tubular reactor were governed by the following factors: Sufficient length was necessary to provide adequate residence time for reaction. The Reynolds number for the reactant stream was to be greater than 5,000 to ensure turbulent flow. Finally, the tube cross-sectional area had to be such that, with the above two conditions satisfied, the tube flow rate did not exceed approximately 25 gal./hr. The solubility limit of diethyl adipate in water placed an upper bound on ester concentration at 0.02 mole/liter.

The temperature of the inlet ester solution (1.5 liters/min.) could be controlled to within 0.2°F. in the range of 80° to 150°F., with a two-mode (proportional plus integral control) pneumatic control system. Inlet shell water was taken directly from the hot water mains. Ester solution and hot water were pumped by bronze gear pumps containing adjustable, spring loaded relief valves connecting outlet and inlet. Sodium hydroxide solution (55 cc./min.) was driven by nitrogen gas above a polyethylene diaphragm in a 13-liter polyethylene-lined steel vessel. All flows were controlled with needle valves.

DEVELOPMENT OF THE MATHEMATICAL MODEL

The saponification of diethyl adipate may be expressed by the following consecutive chemical reactions:



The reaction rates follow the usual second-order rate laws.

$$r_A = -k_1 C_A C_B \quad (3)$$

$$r_{R_1} = k_1 C_A C_B - k_2 C_{R_1} C_B \quad (4)$$

$$r_B = -k_1 C_A C_B - k_2 C_{R_1} C_B$$

Reaction rate constants were measured in both batch and flow systems over the temperature range of 29° to 85°C. Details of these measurements are given in reference 9. The best estimates of activation energies and frequency factor were found to be

$$k_{10} = 4.87 \times 10^6 \text{ liter/(g.-mole) (sec.)}$$

$$E_1 = 10,080 \text{ cal./g.-mole}$$

$$k_{20} = 3.49 \times 10^3 \text{ liter/(g.-mole) (sec.)}$$

$$E_2 = 5,965 \text{ cal./g.-mole}$$

where

$$k_i = k_{i0} \exp(-E_i/RT) \quad (6)$$

Both reactions were found to be exothermic. Measured

heats of reaction were

$$(-\Delta H_1) = 10.8 \text{ kcal./g.-mole}$$

$$(-\Delta H_2) = 16.3 \text{ kcal./g.-mole}$$

Measurements of effective axial dispersion gave values of the dispersion number (D_e/vL) of the order of 0.01. Tichacek (13) has shown that for consecutive second-order reactions occurring in tubular reactors, the fractional decrease in peak conversion to middle product due to axial dispersion is approximately equal to the dispersion number. Hence the effect of axial dispersion was neglected. An attempt was made to fit the nonisothermal reactor concentration and temperature data with a plug-flow model.

Steady state differential material balances on components A and R_1 yield

$$dY_A/dZ = -\alpha \rho^2 k_1 Y_A Y_B \quad (7)$$

$$dY_{R_1}/dZ = \alpha \rho^2 Y_B (k_1 Y_A - k_2 Y_{R_1}) \quad (8)$$

where α is defined by

$$\alpha = \frac{S_T}{G_{Ain}} \frac{C_{Ain}^2}{\rho_{in}} \quad (9)$$

Y_B was determined from an overall material balance as

$$Y_B = Y_{Bin} + (Y_{R_1} - Y_{R_{1in}}) - 2(1 - Y_A) \quad (10)$$

Energy balances on tube and shell fluids yield

$$\frac{dT_T}{dZ} = \left(\frac{1}{W_T C_T} \right) \cdot \{ D_{T_0} U_o (T_S - T_T) + \alpha G_{Ain} Y_B \rho^2 \cdot [(-\Delta H_1) k_1 Y_A + (-\Delta H_2) k_2 Y_{R_1}] \} \quad (11)$$

$$\frac{dT_S}{dZ} = \frac{D_{T_0} U_o}{W_S C_S} (T_T - T_S) \quad (12)$$

To compute U_o , density and viscosity were assumed equal to those of water at the same temperature. The dimensionless plot of Sieder and Tate (12) was used to compute tube and shell side heat transfer coefficients, which were then used to compute the overall heat transfer coefficient U_o . The computed value of U_o was in the range 100 to 700 B.t.u./(hr.) (sq.ft.) (°F.) and varied approximately 20% over the reactor length. In cases where there was no shell flow, the shell passage was blown out with compressed air to reduce the time to reach steady state. A small heat loss then occurred through the shell to the surroundings. This was incorporated into the model by substituting in Equation (12) the expression $U_L(T_{SURR} - T_T)$ for the expression $U_o(T_S - T_T)$. U_L was found experimentally to have a value of 1.76 B.t.u./(hr.) (sq.ft.) (°F.).

PREDICTION OF THE PLUG-FLOW MODEL

Figures 3 and 4 illustrate the agreement between experimental concentration and temperature data, and the predictions of the plug-flow model.

The concentration profiles of reactor run 3 (not shown) were used to determine the rate law constants given in Equation (6). These rate law constants were chosen using nonlinear regression to produce the best fit of the plug-flow model to the experimental data. The rate law constants of Equation (6) were then used with the plug-flow model for subsequent runs. A summary of run conditions discussed here is given in Table 1.

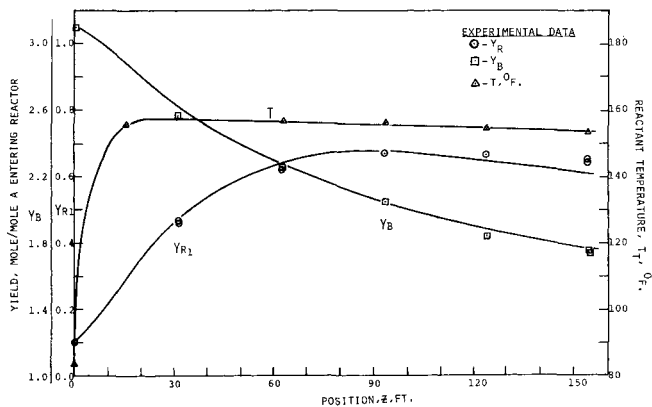


Fig. 3. Run 6: reactor concentration and temperature profile.

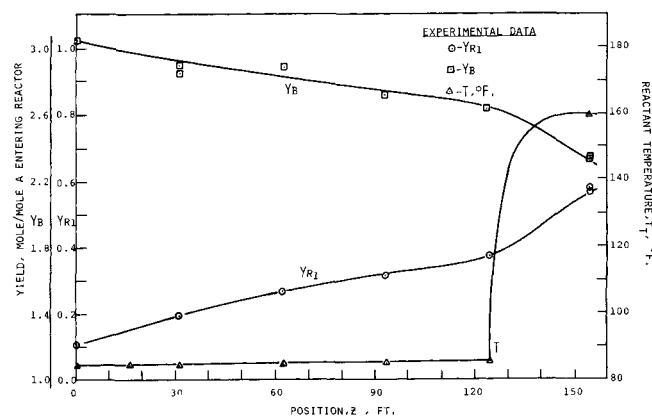


Fig. 4. Run 7: reactor concentration and temperature profiles.

OPTIMAL OPERATION OF THE EXPERIMENTAL REACTOR

To demonstrate optimal operation of the tubular reactor, this study was limited to a single set of controls and a single objective function. The problem posed was: How should the hot water flows in each of the shell sections be set such that steady state conversion of diethyl adipate to monoethyl adipate is maximized at the reactor exit? Inlet shell hot water temperature, reactant temperature, and concentrations were taken as constant. Limitations of the hot water supply system required that no single flow rate exceed 600 lb./hr. The above statements completely defined the problem and were grouped in an algorithm which did the following:

1. Given the following parameters:
 - a. feed concentrations
 - b. feed temperatures
 - c. reaction rate law constants
 - d. heats of reaction
2. Given a set of values of shell hot water flows in the range

$$0 \leq W_{s_i} \leq 600 \text{ lb./hr.}, \quad i = 1, \dots, 5$$
3. Utilize the plug-flow model and the Runge-Kutta method to perform numerical integration of heat and material balances.
4. Calculate the values of exit conversion of monoethyl adipate Y_{R1} .

This procedure was combined with gradient and direct search algorithms to choose the set of shell flow rates subject to

$$0 \leq W_{s_i} \leq 600 \text{ lb./hr.}$$

which maximized Y_{R1} at the reactor exit. The essence of these search techniques is described in the literature (3, 5, 14).

Numerical integration of the four ordinary differential equations using a total of 61 steps required 2 to 3 sec. on the I.B.M. 7090 computer. The optimum set of shell flows was generally found to within 0.01% in less than 50 iterations. The gradient search was faster in reaching the neighborhood of the optimum, but the direct search always obtained a slightly better optimal conversion. The gradient search required between 1 and $(2 + N)$ function evaluations per step ($N = 5$), whereas the direct search required between $(N + 1)$ and $(2N + 1)$ function evaluations. However, the direct search generally required fewer steps, and often the length of each step was larger than that of the gradient search. Doubling the number of integration steps had no appreciable effect on predicted concentration or temperature profiles.

Figure 5 illustrates predicted and measured concentration and temperature profiles which are nearly optimal. That is, the predicted exit conversion of monoethyl adipate is only 0.3% less than the predicted maximum conversion. The reactor was not run with the optimal shell flows partly because of the time required for chemical analysis (24 hr.), and because of turnaround time (24 hr.) at the University of Michigan Computing Center. Had a fast, time-shared computer been available, the latter problem would have been eliminated. The former occurred because only the measured initial concentrations of the previous run (9) were available for the computer program to predict optimal shell flows. The optimal reactor run (10) was then made directly after feedstock sampling. After the results of chemical analysis became available, the numerical search was repeated. Conditions for runs 9 and 10 are shown in Table 1. The optimal controls and final conversion to monoester are shown in Table 2.

The very small difference between optimal exit compositions on a mole ratio basis is due to the small difference in activation energies, 4,000 g.cal/mole, for the first and second saponification reactions. This difference causes the ratio of k_1/k_2 to change by only 1.9%/°C. Had the activation energies been equal, exit concentrations of monoester would differ only due to differences in inlet monoester concentrations.

OPTIMAL OPERATION OF A THEORETICAL TUBULAR REACTOR

To obtain an upper bound on conversion in a tubular reactor of fixed length, consider that the reactor shell is

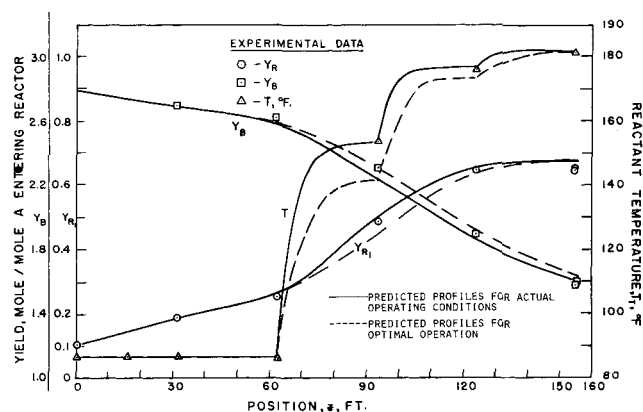


Fig. 5. Run 10: reactor concentration and temperature profiles.

TABLE 1. SUMMARY OF RUN CONDITIONS

Run No.	3	5	6	7	8	9	10
C_A , mole/liter $\times 100$	1.678	1.902	1.737	1.796	1.786	1.718	1.811
Y_{R1}	0.1310	0.1073	0.1023	0.1036	0.1113	0.111	0.102
Y_{R2}	0.00933	0.00438	0.00440	0.00455	0.00320	0.00100	0.0040
Y_B	3.108	2.975	3.098	3.045	2.953	2.960	2.798
T_{Tb} , °F.	81.8	83.0	83.7	84.6	143.8	86.5	86.4
T_{Sib} , °F.	184.3	186.5	184.7	186.6	—	179.6	183.6
Tube flow, lb./hr.	198	198	197	197	194	197	197
Shell flows, lb./hr.							
No. 1	346	0	538	0	0	0	0
No. 2	346	0	0	0	0	392	0
No. 3	346	346	0	0	0	597	436
No. 4	346	346	0	0	0	597	600
No. 5	346	346	0	538	0	597	600

divided into many short lengths, and that the flow in each shell section and its temperature may be adjusted. In this way we can control either the reactant temperature or the heat flux into the reactant fluid at every point along the reactor. Maximization of conversion in this hypothetical reactor is then a variational problem amenable to study with the Pontryagin maximum principle.

Consider first the optimal reactor temperature profile. As a further simplification, assume that bulk density is constant. Component material balances then lead to the required state equations:

$$\frac{dY_1}{dt} = -k_1 Y_1 C_B = f_1(\vec{Y}) \quad (13)$$

$$\frac{dY_2}{dt} = (k_1 Y_1 - k_2 Y_2) C_B = f_2(\vec{Y}) \quad (14)$$

$$C_B = C_{B1} + [Y_2 + 2Y_1 - (Y_{21} + 2)] C_{A1} \quad (15)$$

We ask for the temperature profile along the reactor such that $T_* \leq T \leq T^*$ and Y_2 is maximized at the reactor exit. The Hamiltonian has the form

$$H = \vec{\psi} \cdot \vec{f} = [-\psi_1 k_1 Y_1 + \psi_2 (k_1 Y_1 - k_2 Y_2)] C_B \quad (16)$$

and the adjoint equations have the form

$$\frac{d\psi_1}{dt} = -\frac{\partial H}{\partial Y_1} = C_B k_1 (\psi_1 - \psi_2) - 2H/C_B \quad (17)$$

$$\frac{d\psi_2}{dt} = -\frac{\partial H}{\partial Y_2} = k_2 \psi_2 C_B - H/C_B \quad (18)$$

with boundary conditions

$$\psi_1(t_f) = 0 \quad \psi_2(t_f) = -1 \quad (19)$$

TABLE 2. COMPARISON OF PREDICTED OPTIMAL SHELL FLOWS AND MONOESTER YIELD FOR INITIAL CONDITIONS OF RUNS 9 AND 10

Data from analysis prior to run number	Optimal shell flows, lb./hr.					Y_{R1} (Exit)
	1	2	3	4	5	
9	0	0	435.9	600	600	0.6722
10	0	0	258.9	600	600	0.6719

Write k_2 as a function of k_1 rather than T , and seek k_1 in the region $k_{1*} \leq k_1 \leq k_{1ext}$ along the trajectory such that H is minimized. The minima of H may be found most easily by examining the first and second derivatives of H with respect to k_1 and k_{1ext} (the value of k_1) such that

$$\left. \frac{\partial H}{\partial k_1} = 0 \right\}; \quad k_2 = k_{20} (k_1/k_{10})^{E_2/E_1} \quad (20)$$

$$\frac{\partial H}{\partial k_1} = Y_1 (\psi_2 - \psi_1) - \frac{Y_2 \psi_2 k_{20}}{(k_{10})^{E_2/E_1}} \cdot \frac{E_2}{E_1} \cdot k_1^{\frac{E_2-E_1}{E_1}} \quad (21)$$

$$\begin{aligned} \frac{\partial^2 H_2}{\partial k_1^2} &= \left[\frac{Y_2 \psi_2 k_{20}}{(k_{10})^{E_2/E_1}} \cdot \frac{E_2}{E_1} \cdot \frac{(E_1 - E_2)}{E_1} \cdot k_1^{(E_2-2E_1)/E_1} \right] C_B \quad (22) \end{aligned}$$

$$k_{1ext} = \frac{Y_2}{Y_1} \cdot \frac{E_2}{(E_2 - E_1)} \cdot \frac{E_2}{E_1} \cdot \frac{k_{20}}{(k_{10})^{E_2/E_1}} \cdot k_1^{E_1/(E_1-E_2)} \quad (23)$$

Now consider the various areas of the ψ plane:

1. $\psi_2 > 0, \psi_2 > \psi_1$

k_{1ext} is real and single valued, and $\partial^2 H/\partial k_1^2 < 0$. Therefore H has a minimum at k_{1ext} . Hence

If $k_{1*} \leq k_{1ext} \leq k_1^*$, let $k_1 = k_{1ext}$.

If $k_{1ext} < k_{1*}$, let $k_1 = k_{1*}$.

If $k_{1ext} > k_1^*$, let $k_1 = k_1^*$.

2. $\psi_2 > 0, \psi_2 < \psi_1$

k_{1ext} has no real value and $\partial H/\partial k_1 < 0$. Therefore, to minimize H , let $k_1 = k_1^*$.

3. $\psi_2 > 0, \psi_2 = \psi_1$

Equation (23) is not valid for this case. ($\partial H/\partial k_1 < 0$); therefore let $k_1 = k_1^*$.

4. $\psi_2 \leq 0, \psi_2 > \psi_1$

k_{1ext} has no real value, and ($\partial H/\partial k_1$) is positive. Therefore let $k_1 = k_1^*$.

5. $\psi_2 < 0, \psi_2 < \psi_1$

TABLE 3. VALUES OF PARAMETERS FOR VARIATIONAL PROBLEMS

Reactor residence time = 38 sec.

Initial conditions

$C_A = 0.0175$ g.-mole/liter

$Y_1(0) = 1.0$ mole/mole A entering reactor

$Y_2(0) = 0.1$

$Y_B = 3.0$

$Y_3(0) = T$ - free (determined along with optimal profiles)

k_{1ext} is real, but $(\partial^2 H / \partial k_1^2) < 0$ so that k_{1ext} produces a maximum in H . It is therefore necessary to choose k_1 at the extreme which gives the lower value of H .

6. $\psi_2 < 0$, $\psi_2 = \psi_1$

Since $(\partial H / \partial k_1) > 0$ for all values of \vec{Y} , set $k_1 = k_{1*}$.

7. $\psi_2 = 0$, $\psi_1 > \psi_2$

Since $(\partial H / \partial k_1) < 0$, set $k_1 = k_1^*$.

8. $\psi_1 = \psi_2 = 0$.

This is impossible for then $\psi = 0$, and the required final condition, Equation (7), could not be reached.

To complete the investigation, we must look for the possibility of singular control where H is independent of k_1 for a finite time. From Equation (16) this will be possible only if $\psi_1 = 0$ or $Y_1 = 0$ and $\psi_2 = 0$ or $k_1 Y_1 = k_2 Y_2$ and consequently $H = 0$. At $t = t_f$, $\psi_1 = 0$, $\psi_2 \neq 0$, but it is possible that $k_1 Y_1 = k_2 Y_2$. However, $\psi_1 \neq 0$ so that at $t = t_f$, ψ_1 becomes nonzero. Surely $Y_1 \neq 0$ for t_f finite. H then becomes a function of k_1 and singular control is not possible.

The state and adjoint Equations (1), (2), (5), and (6) were integrated backward using the Runge-Kutta method

by guessing final values on \vec{Y} . These final values were chosen using both direct and gradient search methods to match the known initial conditions $Y(0)$. The optimal control was determined each time derivatives were calculated (four times per step). The parameters used for these problems are given in Table 3.

Figure 6 shows the optimal trajectories which most nearly match the required initial conditions. The optimal temperature profile is of the bang-bang type with a single jump from the lower limit, 28°C., to the upper limit, 85°C. To match the required initial conditions accurately, it was necessary to determine precisely the point of discontinuity. This point was determined to within 10^{-4} sec., whereas the normal set up size for integration was 0.5 sec.

We will now consider a somewhat more realistic problem, and one which has a somewhat simpler solution. In general, it is not the reactant temperature which can be controlled, but the heat flux. We therefore look for the optimal wall heat flux profile in the range $0 \leq q \leq q^*$ which will maximize conversion to monoethyl adipate Y_2 at the reactor exit. The wall heat flux is then linked to reactant temperature and composition by a differential heat balance which becomes the third state equation:

$$\frac{dT}{dt} = \frac{dY_3}{dt} = (a_1 k_1 Y_1 + a_2 k_2 Y_2) C_B + a_3 q \quad (24)$$

where

$$a_1 = (-\Delta H_1) C_{A_i} / \rho C_t$$

$$a_2 = (-\Delta H_2) C_{A_i} / \rho C_t \quad (25)$$

$$a_3 = 4 / (D_i \rho C_t)$$

The material balance equations remain unchanged. The Hamiltonian and adjoint equations then become

$$H = k_1 Y_1 (-\psi_1 + \psi_2 + a_1 \psi_3)$$

$$+ k_2 Y_2 (-\psi_2 + a_2 \psi_3) C_B + \psi_3 a_3 q \quad (26)$$

$$\frac{d\psi_1}{dt} = k_1 C_B (\psi_1 - \psi_2 - a_1 \psi_3) - \frac{2}{C_B} (H - \psi_3 a_3 q) \quad (27)$$

$$\frac{d\psi_2}{dt} = k_2 C_B (\psi_2 - a_2 \psi_3) - (H - \psi_3 a_3 q) / C_B \quad (28)$$

$$\frac{d\psi_3}{dt} = \frac{C_B}{R Y_3^2} [k_1 E_1 Y_1 (\psi_1 - \psi_2 - a_1 \psi_3) + k_2 E_2 Y_2 (\psi_2 - a_2 \psi_3)] \quad (29)$$

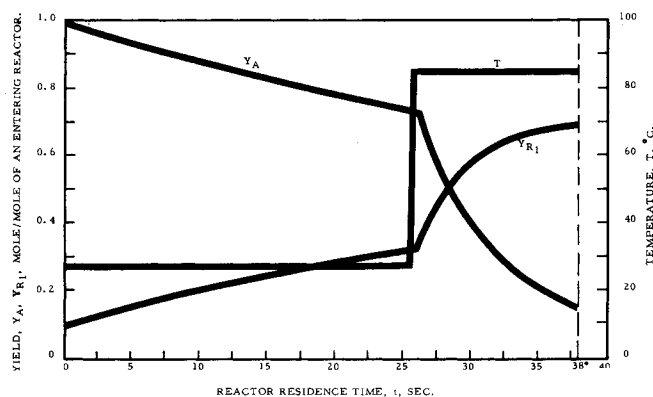


Fig. 6. Optimal trajectories for bounded temperature control.

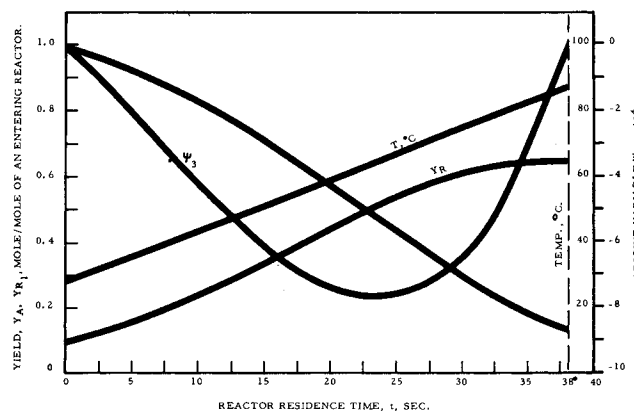


Fig. 7. Optimal trajectories for bounded heat flux control.

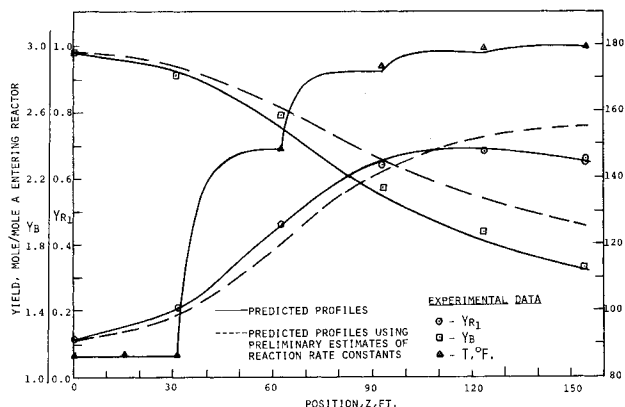


Fig. 8. Run 9: reactor concentration and temperature profiles.

TABLE 4. COMPARISON OF IDEAL AND ACTUAL REACTOR OPTIMIZATIONS

	Predicted	Measured
1. Suboptimal reactor run 10	0.672	0.652
2. Optimal shell flows for conditions of run 10	0.673	—
3. Optimal temperature profile	0.692	—
4. Optimal constrained heat flux profile $0 \leq q \leq 181.1, \text{ cal./}(\text{sec.}) (\text{sq. ft.})$	0.652	—
5. Optimal isothermal operation, $T = 61.8^\circ\text{C.}$	0.613	—

Since Y_2 is to be maximized at the reactor exit, final conditions on $\vec{\psi}$ are

$$\psi(t_f) = [0, -1, 0]' \quad (30)$$

The initial temperature was allowed to be free in which case $\psi_3(0) = 0$. That is, we require the initial temperature and accompanying heat flux profile which will maximize $Y_2(t_f)$ compared with all other inlet temperatures and heat flux profiles.

Since q , the control variable, enters the Hamiltonian linearly, the nonsingular control which minimizes H is apparent:

$$\begin{aligned} \text{If } \psi_3 > 0, \text{ let } q &= 0 \\ \text{If } \psi_3 < 0, \text{ let } q &= q^* \end{aligned} \quad (31)$$

If $\psi_3 = 0$ and $\dot{\psi}_3 \neq 0$, then ψ_3 will become nonzero in the next instant and the above control will apply.

If $\psi_3 = \dot{\psi}_3 = 0$, then q may be chosen at will in the allowable region. In general, this will cause ψ_3 immediately to become nonzero, and the control of Equation (31) would apply. Therefore no change in the trajectories would be apparent due to this instantaneous switching, except that the optimal control might be steered to one of the control boundaries. An alternative is to choose $q = q_{\text{sing}}$ such that $\dot{\psi}_3$ remains zero, thereby keeping $\psi_3 = \dot{\psi}_3 = 0$. This will be possible only if $0 \leq q_{\text{sing}} \leq q^*$. The possibility of singular control is examined in further detail in reference 9.

As in the previous problem, guesses were made on $\vec{Y}(t_f)$ and the set of state and adjoint equations integrated backward in an attempt to match the known initial conditions:

$$Y_1(0) = 1, \quad Y_2(0) = Y_{21} = 0.1, \quad \psi_3(0) = 0$$

The optimal control was computed each time derivatives were calculated.

A comparison of the various optimal solutions is shown in Table 4. The optimal temperature profile gives the highest conversion of all the problems considered, and also gives an upper bound for conversion in reactors described by the plug-flow model, with the same residence time and temperature range. This is true because all other optimal solutions are possible candidates for the solution of the optimal temperature control problem. The choice of a constrained heat flux profile produces a final conversion which is 6% less than that produced with the optimal temperature profile. The heat flux constraint, $0 \leq q \leq 181.1 \text{ cal./}(\text{sec.}) (\text{sq. ft.})$, was chosen so that with full heating the total temperature change along the reactor would be approximately equal to the total temperature change in the jacketed reactor operating optimally. There are certainly sections of the jacketed reactor where the

heat flux is much higher than the average value. Hence the optimal control of the jacketed reactor is a heat flux profile outside the constraints set for the idealized reactor. Best isothermal operation produces the lowest yield of all problems considered.

SUMMARY AND CONCLUSIONS

These comparisons lead to important conclusions regarding the usefulness of the maximum principle for tubular reactor optimization. Since the optimal temperature problem provides an upper bound on yield in real reactors, this is a logical point of comparison for all actual tubular reactor designs. However, for more complex reaction systems, the optimal temperature profile is much more difficult to determine, for the following reason. In the previous analysis, it was necessary to find the control in the allowable control region (either temperature or k_1) which minimized the Hamiltonian H at every point along the reaction path. Success was achieved with reasonably short computing times (1 to 3 min. on the I.B.M. 7090) mainly because minimization of H could be accomplished in an analytical rather than a numerical fashion. That is, an explicit expression was obtained for k_1 which minimized

H for all possible values of \vec{Y} and $\vec{\psi}$. Only the two-point boundary-value problems had to be solved by trial and error. Had a numerical minimization been required at each step of the integration, not only would computing time have increased by a factor of 10 to 20, but the approximations necessary might have caused instabilities which would make numerical solution impossible. Failure to realize this is the major reason for difficulties reported in the literature concerning the usefulness of the maximum principle. In chemical systems in which more than two reactions occur, an analytical determination of temperature to minimize the Hamiltonian will not be possible. However, the optimal constrained heat flux problem will always lead to a Hamiltonian which is linear in the control variable q . The minimization of H will therefore always be possible. The upper and lower limits on heat flux should be set at the minimum and maximum possible in the real reactor. This will guarantee that the choice of heat flux profiles will include all those possible in the real reactor, and will provide an upper bound on exit conversion.

NOTATION

C_i	= concentration of component i , g.-mole/liter
$C_{T,S}$	= tube or shell fluid heat capacity, B.t.u./ (lb.-mole) ($^\circ\text{F.}$)
$D_{T,S}$	= tube or shell diameters, ft.
$E_{1,2}$	= activation energies of two consecutive reactions, cal./g.-mole
G_{Ain}	= molar rate of diester entering reactor, g.-mole/hr.
$k_{1,2}$	= reaction rate constants for first and second saponification reactions, liter/g.-mole/sec.
r	= reaction rate, g.-mole/ (sec.) (liter)
R	= gas constant, cal./ (g.-mole) ($^\circ\text{K.}$)
S_T	= tube cross-sectional area, sq.ft.
T	= absolute temperature, $^\circ\text{K.}$
U_o	= overall heat transfer coefficient between tube and shell fluids based on tube outside area, B.t.u./ (hr.) (sq.ft.) ($^\circ\text{F.}$)
W	= mass flow rate, lb./hr.
Y_i	= mole ratio, mole i per mole of A entering reactor
Z	= axial position, ft.

Greek Letters

- α = defined by Equation (9)
 ρ = density, lb.-mole/cu.ft.
 ψ = adjoint variable in maximum principle formulation

Subscripts

- A = diethyl adipate
B = hydroxyl ion
 R_1 = monoethyl adipate ion
 R_2 = adipate ion
S = shell side
T = tube side
i = inside
in = inlet
o = outside
1, 2 = first and second saponification reactions

LITERATURE CITED

1. Aris, R., "The Optimal Design of Chemical Reactors, A Study in Dynamic Programming," Academic Press, New York (1961).
2. Bilous, O., and N. R. Amundson, *Chem. Eng. Sci.*, **5**, 81-92, 115-126 (1956).
3. Boas, A. H., *Chem. Eng.*, 97-104, (Mar. 1964).
4. Denbigh, K. G., "Chemical Reactor Theory," Cambridge Univ. Press (1965).
5. Hooke, R., and T. A. Jeeves, *J. Assoc. Computing Machinery*, **8**, (2), 212-219 (Apr. 1961).
6. Horn, F., *Chem. Eng. Sci.*, **14**, 77-88 (Jan. 1961).
7. Katz, S., *Ann. N. Y. Acad. Sci.*, **84**, 441-478 (1960).
8. Kramers, H., and K. Westerterp, "Elements of Chemical Reactor Design and Operation," Netherlands Univ. Press (1963).
9. Newberger, M. R., Ph.D. thesis, Univ. Michigan, Ann Arbor (1967).
10. Pontryagin, L. S., et al., "Mathematical Theory of Optimal Processes," Wiley, New York (1962).
11. Siebenthal, C. E., and R. Aris, *Chem. Eng. Sci.*, **19** (10) 747-761 (Oct. 1964).
12. Sieder, E. N., and G. E. Tate, *Ind. Eng. Chem.*, **28**, 1429-1435 (1936).
13. Tichacek, L. J., *AIChE J.*, **9** (3), 394-399 (May 1963).
14. Zellnick, H. E., N. E. Sondack, and R. S. Davis, *Chem. Eng. Progr.*, **58** (8), 35-41 (Aug. 1962).

Manuscript received June 9, 1969; revision received February 2, 1971; paper accepted February 3, 1971.

Hydrodynamic Measurements for Imperfect Mixing Processes: Newtonian Fluids

DAVIS W. HUBBARD and HARISH PATEL

Department of Chemistry and Chemical Engineering
Michigan Technological University, Houghton, Michigan 49931

The response of a continuous flow mixing system to a step change in an input variable is discussed from the standpoint of dimensional analysis. This idea is presented as an alternative to using zone models for predicting residence time distributions in systems where imperfect mixing occurs.

Mixing experiments were performed in a cylindrical flat bottomed tank geometrically similar to tanks commonly used for industrial processes. The response of the system to a step change in feed concentration was observed. Initially the tank contained a salt solution. At the start of an experiment, a stream of salt-free diluent was introduced at the top of the tank and a stream of the salt solution was drained from the bottom, keeping the liquid volume in the tank constant. The salt concentration in the output stream was measured continuously after the start of the experiment.

The experimental results are correlated in terms of dimensionless variables, and the variables affecting the mixing process most strongly are determined. The results show that variations in throughput rate or in impeller shape or rotational speed affect the mixing process much more than does impeller position. The data are also compared with models proposed by other authors, and the model constants are evaluated.

Recently, experimenters have been studying stirred-tank systems from the fundamental point of view, using the principles of fluid mechanics, energy transport, and mass transport to predict the behavior of the system. Several authors (1, 2) have reported detailed velocity profiles within the mixing tank itself and have related the profiles

to the impeller speed, fluid properties, and geometric variables. Logical extensions of such work would be to determine temperature and concentration distributions in the stirred tank and correlate the data in a similar manner. Other workers (3 to 13) have analyzed the stirred-tank system from a macroscopic viewpoint. Power requirements have been related to geometric and process variables using this approach, and energy and mass transfer processes have been studied. Many of these studies have been carried out using a continuous flow stirred tank. A schematic flow

Correspondence concerning this article should be addressed to Davis W. Hubbard. Harish Patel is with Dow Chemical Co., Midland, Michigan 48640.